Title

Principles of dimer-specific gene regulation revealed by a comprehensive characterization of NF-κB family DNA binding

Journal

Nature Immunology, 13(1)

ISSN

1529-2908

Authors

Siggers, Trevor
Chang, Abraham B
Teixeira, Ana
et al.

Publication Date

2012

DOI

10.1038/ni.2151

Peer reviewed

Nat Immunol. Author manuscript; available in PMC 2012 July 01.

Published in final edited form as:
Nat Immunol. ; 13(1): 95–102. doi:10.1038/ni.2151.

Principles of dimer-specific gene regulation revealed by a comprehensive characterization of NF-κB family DNA binding

Trevor Siggers[1,7], **Abraham B Chang**[2,7], **Ana Teixeira**[3], **Daniel Wong**[3], **Kevin J Williams**[2], **Bilal Ahmed**[1,4], **Jiannis Ragoussis**[3], **Irina A Udalova**[5], **Stephen T Smale**[2], and **Martha L Bulyk**[1,4,6,*]

[1]Division of Genetics, Department of Medicine, Brigham & Women's Hospital and Harvard Medical School, Boston, Massachusetts, USA

[2]Molecular Biology Institute and Department of Microbiology, Immunology, and Molecular Genetics, University of California Los Angeles, Los Angeles, CA, USA

[3]Wellcome Trust Centre for Human Genetics, Oxford University, Oxford, UK

[4]Harvard-MIT Division of Health Sciences and Technology, Harvard Medical School, Boston, Massachusetts, USA

[5]Kennedy Institute of Rheumatology, Imperial College, London, UK

[6]Department of Pathology, Brigham & Women's Hospital and Harvard Medical School, Boston, Massachusetts, USA

Abstract

The unique DNA-binding properties of distinct NF-κB dimers are known to influence the selective regulation of NF-κB target genes. To gain a stronger appreciation for these dimer-specific differences, we have combined protein-binding microarrays (PBM) and surface plasmon resonance (SPR) to evaluate DNA sites recognized by eight different NF-κB dimers. We observed three distinct binding-specificity classes and provide insight into mechanisms by which dimers might regulate distinct sets of genes. We identified many new non-traditional κB site sequences and highlight an under-appreciated plasticity of NF-κB dimers in recognizing κB sites with a single consensus half-site. This study provides a database that will be of broad utility in efforts to identify NF-κB target sites and uncover gene regulatory circuitry.

Introduction

The transcription factor NF-κB regulates a broad range of genes central to the body's immune and inflammatory responses[1-4]. NF-κB represents homo- and heterodimers of five different family members: c-Rel (REL), RelA/p65 (RELA), RelB (RELB), p50/p105 (NFKB1), and p52/p100 (NFKB2)[5-7]. Studies of knockout mice have revealed that each NF-κB family member carries out unique biological functions[8-11]. At a molecular level, DNA-

*Correspondence should be addressed to M.L.B. (mlbulyk@receptor.med.harvard.edu). .
[7]These authors contributed equally to this work.

Author Contributions

T.S. designed and performed PBM experiments, and performed ChIP data analysis. T.S. and B.A. performed PBM data analyses. A.B.C. and K.J.W. made murine protein samples. A.B.C. performed SPR experiments. A.T., D.W., J.R. and I.A.U. provided human protein samples. The manuscript was written by T.S., A.B.C., S.T.S. and M.L.B.

Methods

Methods and associated references are available in the online version of the paper at http://www.nature.com/natureimmunology
Note: Supplementary information is available on the Nature Immunology website.

Europe PMC Funders Author Manuscripts

binding differences of individual NF-κB dimers have been linked to dimer-specific roles in gene regulation[6,7]; however, much remains unclear regarding the full scope of these differences and how they affect dimer-specific functions *in vivo*.

Protein-DNA crystal structures[6,12] and DNA-binding studies[12-14] have led to a basic partition of the NF-κB family members: p50 and p52 recognize a 5-bp 5′-GGGRN-3′ half-site, while c-Rel, RelA, and RelB recognize a 4-bp 5′-GGRR-3′ half-site (R = {A,G}; N={A,C,G,T}). These half-sites, separated by a 1-bp spacer, led to the consensus heterodimer binding site (i.e., κB site) 5′-GGGRN(Y)YYCC-3′[15]. Despite the appeal of this paradigm, reports of additional dimer-specific DNA-binding preferences[16] and non-canonical NF-κB binding site sequences[5,17] suggest complications to this simple picture.

Dimer-specific DNA recognition provides a mechanism to disentangle the *in vivo* functions of NF-κB heterodimers and closely related homodimers. One such example is specific recognition of the murine BLC-κB site reported for the RelB:p52 heterodimer – the primary dimer mediating the alternative NF-κB signaling pathway[16,18-20]. However, contradictory results for RelB:p52-specific binding have been reported[21]. Binding of other NF-κB dimers to non-canonical binding site sequences has also been reported and suggests plasticity in DNA binding. Examples include the c-Rel target site in the *Il12b* gene promoter (5′-GGGGAATTTT-3′)[17] and the CD28 response element (CD28RE) from the *Il2* and *Csf2* gene promoters (5′-GGAATTTCT-3′)[5]. Both sites deviate from the consensus sequence and score poorly according to the standard position weight matrices (PWMs) derived from binding site selections[13]. Structural analyses of NF-κB dimers in complex with different κB site sequences have also demonstrated a striking plasticity in the amino acid-base interactions[12]. Together, these observations suggest that the consensus sequence and PWM descriptions of NF-κB DNA binding are too limited.

To address these issues, we have used the protein-binding microarray (PBM) technology[22-24] and surface plasmon resonance (SPR) to perform an unbiased characterization of potential κB binding site sequences using multiple NF-κB dimers. Previous large-scale analyses of NF-κB DNA-binding have been biased either to certain κB site sequences[14,25] or to only the few highest affinity sites[13]. We observed three distinct NF-kB binding-specificity classes, identified many new non-traditional κB site sequences, and highlight an under-appreciated plasticity of NF-κB dimer binding for shorter kB sites with one consensus half-site. We provide a novel and rich dataset and anticipate that it will prove useful for genomic analysis of NF-κB regulatory elements and the interpretation of *in vivo* binding experiments. The dataset plus online tools with DNA sequence search capabilities are provided online (http://thebrain.bwh.harvard.edu/nfkb).

Results

Designing an NF-κB-specific protein-binding microarray

To examine the DNA-binding specificities of NF-κB dimers in a systematic and unbiased manner, we utilized PBM technology. PBMs are double-stranded DNA microarrays that allow the *in vitro* characterization of protein binding to tens of thousands of unique DNA sequences in a single experiment[24,26,27]. The universal PBM (uPBM) developed previously[23] allows a comprehensive, unbiased assessment of protein-DNA binding to all ungapped and gapped 8-bp sequences. We carried out uPBM experiments with six human and mouse NF-κB dimers (c-Rel:c-Rel, RelA:RelA, p52:p52, p50:p50, c-Rel:p50, RelB:p52) to perform an initial, comprehensive survey of potential κB site sequences. DNA binding site motifs derived from the uPBM experiments were in excellent agreement with published SELEX data on cRel:cRel, RelA:RelA and p50:p50 homodimers[13] (Supplementary Fig. 1), demonstrating highly specific binding in our assay.

The uPBM platform assesses binding to 8-bp sequences; however, the canonical NF-κB binding site (κB site) is 10-bp long[6,7]. Therefore, we created a custom NF-κB PBM containing 10-bp sequences prioritized according to the uPBM 8-bp data (see Supplementary Methods). We compiled the 1,000 top-scoring 10-bp sequences determined for the six NF-κB dimers into a list of 3,285 non-redundant sequences that represent the top-scoring set of potential κB site sequences. These 10-bp κB sites were incorporated into a custom NF-κB PBM with each site situated within constant flanking sequence (Fig. 1a, see Methods).

We initially examined the binding of RelA:p50 to our custom NF-κB PBM. To assess significance of the results, the natural log of the median PBM signal intensity of each 10-bp site was transformed into a z-score using the scores from 1,200 randomly chosen 10-bp sites as a background distribution (Fig. 1b; see Methods). Many potential κB sites, including a set of validated κB sites, scored significantly higher than the background distribution (z-score > 4), demonstrating that the custom PBMs reveal the specific DNA binding sites of NF-κB dimers. Thus, our custom NF-κB PBM provides a unique platform to assess the DNA-binding specificities of different NF-κB dimers for a large set of potential κB site sequences.

Three distinct DNA binding classes

To examine the DNA-binding preferences of different NF-κB dimers, we performed custom NF-κB PBM experiments for ten dimers from mouse or human. We compared the DNA-binding specificities of different dimers by correlating their κB site z-scores. Hierarchical clustering revealed that the NF-κB dimers separated into three distinct classes: p50 or p52 homodimers; heterodimers; and c-Rel or RelA homodimers (Fig. 1c). This subdivision is similar to the basic division of the NF-κB family members into two subclasses based on protein sequence of the Rel-homology domains: p50 and p52 (subclass 1); c-Rel, RelB and RelA (subclass 2). The common binding specificity observed for the heterodimers suggests a canonical DNA-binding contribution from members of each NF-κB subclass.

To highlight the differences between these three NF-κB classes, we constructed a representative DNA binding site motif for each class (Fig. 1d; Supplementary Fig. 2 for all individual motifs). We identified different DNA binding site motif lengths for each class: 9-bp for c-Rel and RelA homodimers; 10-bp for heterodimers; 11- or 12-bp for p50 and p52 homodimers. We note that while our custom NF-κB PBM was designed to assay binding to a large collection of 10-bp sequences, our *de novo* motif finding approach arrived at a longer motif for p50 and p52 homodimers; length preferences are examined more directly below. The 10-bp motif for the heterodimer class is in excellent agreement with the known NF-κB consensus sequence 5′-GGGRNWYYCC-3′, demonstrating that we correctly identified the known high-affinity binding sites. The variant 9-bp and 11-bp motifs for the c-Rel,RelA and p50,p52 homodimer classes, respectively, also agree with the reported DNA-binding preferences of these different homodimers[6]. A comprehensive overview of the binding landscape for all dimers to the 10-bp κB sites is provided (Supplementary Fig. 3a), along with example genomic regions in which our PBM data are used to annotate dimer preferences for putative κB sites (Supplementary Fig. 3b,c).

In our pair-wise comparisons, all heterodimers exhibit a common DNA-binding specificity. Of particular interest was our observation that RelB-containing heterodimers exhibit DNA-binding specificity similar to that of c-Rel- and RelA-containing heterodimers. The biological significance of this finding is discussed below (see Discussion).

Dimer preferences for traditional and non-traditional κB sites

Dimer-specific DNA-binding preferences provide a mechanism for NF-κB dimers to target distinct binding sites, and thus to regulate distinct target genes. We observed the most distinct DNA-binding preferences (the lowest z-score correlation) between members of the two homodimer classes (Fig. 1c). To investigate these differences further, we compared the binding specificities of the most dissimilar dimers: p50:p50 and c-Rel:c-Rel (z-score correlation = −0.13) (Fig. 2a). We observed many off-diagonal features that correspond to sites bound preferentially by one of the dimers ('dimer-preferred' κB sites).

To identify sequence features that could explain the relative dimer preferences, we examined the c-Rel:c-Rel-preferred κB sites (κB sites with p50:p50 z-score < 2 and c-Rel:c-Rel z-score > 4). We found that a majority had a strong 5′-HGGAA-3′ half-site (Fig. 2a, red dots). Many of these sequences conform to the canonical c-Rel,RelA-preferred 9-bp binding site with two 5′-HGGAA-3′ half-sites separated by a 1-bp spacer[12,28]. However, we also found many non-traditional κB site sequences with only one 5′-HGGAA-3′ half-site. We use the term "non-traditional" in lieu of "non-canonical" to avoid potential confusion with variant κB sites (referred to as non-canonical) reported to be downstream of the non-canonical NF-κB signaling pathway[16]. Non-traditional sites are defined as sites that score poorly by the widely used NF-κB PWMs[13,29] (see Supplementary Methods); examples include CD28RE from the *Il2* and *Csf2* gene promoters (5′-GGAATTTCT-3′, c-Rel:c-Rel z-score = 8.5) and the κB site from the murine *Plau* gene promoter (5′-GGAAAGTAC-3′, c-Rel:c-Rel z-score = 12.9)[5]. We also found that a motif constructed from the c-Rel:c-Rel-preferred κB sequences exhibited a strongly degenerate half-site (Fig. 2b). Therefore, while the highest scoring c-Rel:c-Rel-preferred sites are pseudo-symmetric (Fig. 1d), a large number of non-traditional, c-Rel:c-Rel-preferred sites (and RelA:RelA-preferred, Supplementary Fig. 4) scored significantly above background yet have only a single canonical 5′-HGGAA-3′ half-site.

Examining the p50:p50-preferred κB sites (p50:p50 z-score > 4, c-Rel:c-Rel z-score < 2), we found a number of κB sites with a G-rich 5′ half-site. Highlighting the κB sites that conform to the pattern 5′-GGGGGNNNNN-3′ (Fig. 2a, yellow dots), we observed a strong p50:p50 preference, although a subset of the sites is also bound well by c-Rel:c-Rel (discussed further below). A motif constructed from the G-rich sites bound well by p50:p50 (z-score > 4) exhibits a 5′-GGGGG-3′ half-site and a degenerate 3′ half-site (Fig. 2b), although a moderate preference for adenine and thymine bases 3′ to the G-run was observed. Therefore, similar to the c-Rel:c-Rel-preferred sites, we observed statistically significant binding to a large group of κB sites defined by a single half-site sequence.

To ensure that the observed dimer-specific binding to non-traditional κB sites is not an artifact of our PBM approach, we examined binding to a set of traditional and non-traditional κB sites using SPR (Figs. 2b-d, Supplementary Fig. 5). Due to the very fast on-rates (K_{on}) of some dimers, we were unable to obtain reliable K_{on} measurements. However, we were able to obtain reliable off-rate (K_{off}) values and found excellent agreement between the SPR-determined K_{off} values and our PBM-determined z-scores (Figs. 2d,e). These results are consistent with previous reports[25] showing differential off-rates as the major contributor to binding affinity differences between κB sites. Our data demonstrate that our PBM-determined z-scores reflect equilibrium binding measurements and lend further support for the potential regulatory significance of the numerous non-traditional κB sites in our dataset.

Dimer preferences for κB sites of different lengths

DNA binding studies[13] and X-ray crystal structures[6,12] have revealed different κB site lengths for c-Rel,RelA homodimers (9 bp), heterodimers (10 bp), and p50,p52 homodimers (11 bp). These length preferences are consistent with the DNA binding site motifs we determined for each dimer class (Fig. 1a). However, in light of the number of non-traditional binding sites in our dataset, we sought to determine whether binding site length preferences depend on the binding site sequence itself.

We examined how the DNA bases flanking 10-bp κB sites affect the binding to different dimers. Since p50:p50 binds an 11-bp site, we expected to observe a strong effect due to flanking base identity. We measured binding by PBM experiment to all 16 κB site variants in which the bases immediately 5′ and 3′ to the 10-bp site were exhaustively sampled (Fig. 3a). Examining the binding of p50:p50, RelA:p50 and c-Rel:c-Rel to traditional κB site sequences, we observed improved binding by p50:p50 and RelA:p50 with the addition of 5′ guanine to one strand (Fig. 3a, columns 1 and 2). These differences are readily understood in terms of the known half-site preferences, with high-affinity binding occurring on 11-bp sites with symmetrically opposed, optimal 5-bp half-sites: 5′-GGGGA(A)TCCCC-3′ and 5′-GGGAA(A)TTCCC-3′. However, for p50:p50 the highest-affinity binding occurred with 5′ guanines flanking both half-sites, demonstrating a preference beyond the 5-bp half-site and showing that a 12-bp site can be differentiated from an 11-bp site.

In contrast, we observed that binding of all three dimers was unaffected by the identity of the bases flanking non-traditional κB sites (Fig. 3a, columns 3 and 4). This suggested a different mode of protein-DNA interaction for non-traditional κB sites. To delimit their lengths, we used our PBM dataset to examine binding to shorter κB sites. For example, to interrogate binding to a 9-bp sub-sequence of the 5′-GGGGAATTTT-3′ site, we examined binding to the four κB sites in our dataset of the form 5′-NGGGAATTTT-3′. Binding of p50:p50 and RelA:p50 was insensitive to base identity at position 5 (positions numbered as $5'\text{-}G_{-5}G_{-4}G_{-3}A_{-2}A_{-1}T_{+1}T_{+2}T_{+3}T_{+4}T_{+5}\text{-}3'$) and only moderately sensitive to the base identity at position −5 (Fig. 3b). Therefore, the length of this non-traditional site is 8 to 9 bp (5′-gGGGAATTT-3′), which differs considerably from the 9- to 11-bp traditional κB site sequences (Fig. 3a). In contrast, c-Rel:c-Rel binding is insensitive to positions −5 and −4, but sensitive to base identity at position 5, demonstrating a similarly short 8-bp length but to a different sub-sequence (5′-GGAATTTT-3′). The same preferences were observed for the 5′-GGGGGTTTTT-3′ site (Supplementary Fig. 6). Our data suggest that a fundamentally different mode of binding mediates the recognition of traditional versus non-traditional sites and that this translates into κB sites of different lengths. Furthermore, we observed that the length of the binding site is dimer-specific.

We analyzed the role of flanking bases to 17 additional κB sites and similarly found that 5′ guanine bases were the most predictive of increased binding affinity for all NF-κB dimers, and that the effect of a 5′ guanine was dependent on the G-content in adjacent bases. We generated a linear model to predict the PBM scores for all 12-bp κB sites based on our set of 10-bp κB sites (see Supplementary Methods). We demonstrate the efficacy of this extended dataset below in our comparison of PBM data with chromatin immunoprecipitation (ChIP) data, and make the full dataset available for use in genomic analysis (see Supplementary Data).

Affinity versus specificity of c-Rel and RelA homodimers

The Rel homology regions (RHRs) of c-Rel and RelA are more similar to each other than are the RHRs of any other pair of NF-κB family members[30]. *In vitro* DNA-binding studies have demonstrated highly similar binding specificities, although c-Rel homodimers appear

to bind a broader range of κB site sequences than RelA[13]. We observed highly correlated binding of c-Rel and RelA homodimers over our large set of ~3,300 κB sites (Figs. 1,3 and Supplementary Fig. 2). Despite these similarities, c-Rel and RelA can elicit distinct biological functions *in vivo*[6,17]. c-Rel homodimers can preferentially activate the mouse *Il12b* gene by binding non-traditional NF-κB sites with much higher affinity than RelA homodimers[17]. Forty-six amino acids within the c-Rel RHR were found to be responsible for the enhanced binding affinity, and a chimeric RelA protein containing these 46 residues rescued *Il12b* expression in *cRel*$^{-/-}$ macrophages.

To determine the relationship between our PBM profiles and binding affinity, SPR was performed with six different DNA sequences. For all sequences tested, except for one that bound poorly to both dimers, we observed much slower dissociation rates (K_{off}) for c-Rel homodimers than for RelA homodimers (Table 1). Importantly, swapping these 46 residues of the c-Rel RHR domain into RelA (protein RelA/N3,4) led to substantially slower dissociation rates (Table 1). RelA/N3,4 homodimers also exhibited a binding specificity that correlated more closely with c-Rel homodimers (Pearson $r = 0.87$) than with RelA homodimers (Pearson $r = 0.82$) (Fig. 4). However, these specificity differences are subtle in comparison to the global difference in binding affinity distinguishing c-Rel from RelA homodimers (median fold difference of 8.7 for c-Rel, RelA K_{off} values). Thus, while the DNA-binding specificities of RelA and c-Rel homodimers are highly correlated, c-Rel homodimers have much slower off-rates than RelA homodimers, resulting in a higher overall affinity and contributing to the selective regulation of c-Rel-dependent genes.

These results raised the question of whether binding affinities might discriminate other NF-κB dimers with correlated binding specificities. We performed SPR experiments with the six different DNA sequences using mouse p50:p50 homodimers and c-Rel:p50, RelA:p50, RelB:p50 and RelB:p52 heterodimers (Supplementary Table 1). The results failed to reveal differences of the same magnitude as those found for c-Rel and RelA homodimers. The most notable difference was that c-Rel:p50 heterodimers exhibited slower off-rates with some DNA sequences than the other heterodimers. Although the magnitudes of these differences were smaller than those observed with c-Rel and RelA homodimers (median K_{off} fold difference of 8.7 for the c-Rel, RelA homodimer, versus pairwise heterodimer differences ranging from 1.1 to 5.0), the results raise the possibility that enhanced binding affinity allows c-Rel:p50 heterodimers to selectively regulate some genes.

Comparison with *in vivo* binding data

We examined the relationship between our PBM-derived binding data and available genome-scale ChIP datasets on *in vivo* occupancy of RelA and p50[31-33]. We found highly significant enrichment for high-scoring PBM-determined κB site sequences within ChIP-enriched (i.e., dimer-bound) regions (Supplementary Fig. 7). Moreover, we found significant enrichment when traditional κB sites were masked from the genomic sequence. These results demonstrate that both traditional and non-traditional κB sites in our PBM dataset represent binding sequences utilized *in vivo*.

To determine whether PBM-determined dimer-specific differences correlate with dimer-specific binding differences *in vivo*, we examined an NF-κB ChIP dataset[33] in which ChIP-chip was performed on LPS-stimulated human macrophages for all five NF-κB proteins. Focusing on p50 binding, which had the largest number of bound regions, we separated regions into those bound by p50 only (regions bound by p50:p50 homodimers, Fig. 5a) and those also bound by at least one of RelA, c-Rel or RelB (regions bound by p50 heterodimers or multiple dimers, Fig. 5a). This analysis allowed us to examine whether particular κB sequences distinguish regions bound only by p50:p50 homodimers and whether our PBM data for different dimers capture these sequence differences.

The ~8,000 human promoter regions in the ChIP dataset[33] were scanned with our PBM-determined 12-bp κB site sequences and assigned the z-score of the top-scoring κB site (see Supplementary Methods). Receiver-operating-characteristic (ROC) curve analyses were performed to quantify whether the p50-bound regions (true positives) scored more highly than the unbound regions (true negatives). We observed strong area under the ROC curve (AUC) enrichment scores for all three dimers tested (Fig. 5b-d). However, strikingly, we observed that p50:p50 PBM data yielded significantly higher enrichment scores for the regions bound only by p50 than for the regions bound by additional NF-κB members (AUC=0.84 versus 0.67, Fig. 5b). This was not the case for the RelA PBM data, which showed no discrimination between the two types of regions (Fig. 5d). This demonstrates that κB sequence features can discriminate the p50-specifically bound regions, and that these features correlate best with p50:p50 homodimer PBM data. The same analysis performed with PBM-determined 10-bp or 11-bp κB sites did not show the same discriminatory capacity for p50:p50 (data not shown) suggesting that the p50-bound sites are discriminated primarily by p50:p50 preferences for 12-bp long κB sites. These results demonstrate that the PBM-derived, dimer-specific binding differences relate directly to dimer-specific binding differences *in vivo*.

Discussion

A complete understanding of NF-κB dimer DNA-binding specificities and affinities will provide critical insight into mechanisms available for dimer-specific function in the cell. In this study, we examined the DNA-binding preferences of ten NF-κB dimers from mouse and human to a wide-ranging set of 3,285 potential κB site sequences. We anticipate that this large and detailed dataset of κB sites will prove useful for analyses of NF-κB regulatory elements at a genome scale.

Our results have immediate biological and mechanistic implications for each of the three dimer classes (Table 2). For the c-Rel and RelA homodimers, one major finding is that c-Rel homodimers bind with substantially higher affinity than RelA homodimers to all kB sites, despite highly correlated binding profiles. This suggests an affinity-dependent mechanism for discriminating these homodimers where c-Rel homodimers out-compete RelA homodimers for κB sites *in vivo* on the basis of DNA binding affinity. Under these conditions, RelA homodimers will not preferentially bind to any κB sites. Therefore, to selectively regulate genes in cells that also express c-Rel homodimers (primarily hematopoietic cells), RelA homodimers need to rely on mechanisms other than selective DNA-binding, such as RelA-dependent co-activator interactions[34,35].

For the heterodimer class, the most important biological and mechanistic implication of our results is that the selective functions of each heterodimer may not be achieved via dimer-specific recognition of κB motifs in target genes. The PBM data for all heterodimers correlated closely, indicating that they recognize the same sequences. It is especially noteworthy that binding data for RelB:p52 correlated closely with those of the other heterodimers. It has been reported that RelB:p52, but not RelB:p50 and RelA:p50, can bind well to the non-traditional murine BLC-kB site[16]. More recently, it was reported that RelB:p52 is less discriminatory than RelA:p50 and can bind to a broader set of κB site sequences[20]. Binding sites unique to RelB:p52 – the primary dimer activated in response to the alternative NF-κB pathway[18,19] – would provide a mechanism for cells to differentiate target genes of the alternative NF-κB pathway from those of the classical pathway activating RelA:p50[6].

However, additional studies report that RelB:p52 and RelA:p50 share highly similar binding specificities, with no clear preference exhibited by RelB:p52[21]. We found that RelB:p52 and

RelB:p50 do not differ significantly in their DNA-binding preferences (see Supplementary Discussion). Furthermore, we now extend this to include all NF-κB heterodimers, demonstrating that NF-κB heterodimers exhibit common binding preferences to the ~3,300 κB site sequences examined in this study. Modest binding differences reported for heterodimers[20] may be below the resolution of our approach and may prove functionally important *in vivo* and will need to be examined in greater depth in the future. However, this work and others[21] suggest that the regulation of distinct sets of genes by different heterodimers is likely achieved primarily through alternative mechanisms, such as dimer-specific interactions with co-regulatory proteins[34], dimer-specific synergy with other transcription factors, or dimer-specific conformational differences[20,36,37].

For the p50 and p52 homodimers, we defined a subset of κB site sequences bound preferentially by these homodimers. Importantly, these sequences include a novel G-rich p50 homodimer recognition motif found upstream of the IFN-inducible *Gbp1* gene (5′-GGGGGAAAAA-3′, p50:p50 z-score = 6.2; c-Rel:c-Rel z-score = 4.5) shown to mediate p50 homodimer-dependent repression[38]. This suggests that many other non-traditional, G-rich p50:p50-preferred κB sites in our dataset may similarly function as p50:p50-specific target sites *in vivo*.

In addition to the broad principles summarized above, our results highlight additional levels of complexity in NF-κB-DNA interactions. First, we observed that DNA binding site motifs for significantly bound sites exhibited one strong half-site but a degenerate preference for the opposing half-site (Fig. 2). This is in contrast to more symmetric motifs derived from the highest affinity κB sites (Fig. 1). Second, we observed that non-traditional κB sites appear to be shorter (8- to 9-bp long) than traditional κB sites (9- to 11-bp long). These findings suggest a more modest requirement for a κB site: one traditional half-site sequence recognized via a stereotyped pattern of amino acid-base contacts, with a second half-site that can exhibit considerable plasticity. These results are consistent with structural analyses showing considerable plasticity in both the global conformation of the protein-DNA complex and the amino acid-base contacts mediated by the dimer subunits[12,28,39]. Analyses of c-Rel and RelA homodimers bound to different κB sequences revealed stereotyped amino acid-base interactions with the consensus 5′-GGAA-3′ half-site common to each structure, but highly variable contacts with the half-site sequences that differed between the structures. We propose that structural plasticity afforded by the ability of NF-κB dimers to bind to many κB sites with only a single strong half-site provides a mechanism to partially disentangle DNA binding from structural conformation. In turn, this may allow increased structural diversity and the potential for allosteric mechanisms in transcriptional control as have been reported in several cases[36,37].

In addition to highlighting the challenge of understanding how DNA sequence may influence NF-kB conformation and the functional consequences of NF-kB binding, our results emphasize the importance of the relationship between binding specificity, affinity and function. Our dataset reveals NF-κB binding to a remarkably diverse range of sequences, and suggests that many functionally important sequences (e.g., the *Il2* CD28 RE) may diverge considerably from the optimal κB site. Furthermore, we observed highly overlapping binding specificity of NF-kB dimers and considerable potential for competitive binding. It is well established that, in reporter assays, high-affinity binding sites for NF-κB and other factors lead to stronger transcription than low-affinity sites[40]. However, in a physiological setting within the context of native chromatin, it is not known whether an affinity threshold must be achieved for function, whether a simple relationship exists between affinity and transcriptional output, or what role the effects of co-regulatory proteins and other DNA-bound transcription factors will play. The results reported here provide a further step toward addressing these fundamental questions. Unlike basic consensus

sequences and PWMs, which reveal preferences at each position of a recognition motif, data provided by PBMs and other high-throughput methods[41,42] reveal preferences throughout the continuum of possible binding sequences. These datasets will be invaluable for detailed analyses of the DNA sequence-dependence of transcriptional regulatory control.

Supplementary Material

Refer to Web version on PubMed Central for supplementary material.

Acknowledgments

This work was funded by NIH grant # R01 HG003985 to M.L.B., HFSP grant # RGY0085/2005-C to M.L.B., NIH grant # R01 AI073868 to S.T.S., FP7 Collaborative Project Model-In grant #222008 to J.R. and I.U., support from the M.R.C. to J.R. and I.U., and support from Wellcome Trust grant # 075491/Z/04 to J.R. A.C. was funded by NIH grant # T32 CA009120, and B.A. was funded by the i2b2/HST Summer Institute in Bioinformatics and Integrative Genomics NIH grant # U54 LM008748. We thank G. Natoli (European Institute of Oncology, IFOM-IEO Campus), M. Pasparakis (University of Cologne), and L. Giorgetti (European Institute of Oncology, IFOM-IEO Campus) for helpful discussions.

APPENDIX

Methods

Preparation of protein samples

Mouse sequences for RelA, c-Rel, p50, p52, and RelB were cloned into a modified pET11a expression vector for purification. Constructs contained the Rel-homology region (RHR) of each subunit: RelA (1-314 a.a.), c-Rel (1-282 a.a.), p50 (1-429 a.a.), RelB (1-400 a.a.). The p50 subunit had a C-terminal FLAG tag. Proteins were expressed in BL21 (DE3) *Escherichia coli* cells (0.1 mM isopropyl β-D-1-thiogalactopyranoside (IPTG) induction) for 16 h at 25°C. Heterodimer subunits were co-expressed using a bicistronic expression plasmid[43]. Protein purification was performed on a Q-Sepharose High Performance anion exchange column (GE Healthcare) and a SP Sepharose High Performance cation exchange column (GE Healthcare) and analyzed by SDS-PAGE and EMSA. The final purified protein samples were then frozen in aliquots in a storage buffer of 50 mM Tris-HCl, pH 8.0 150 mM NaCl, 5 mM DTT, and 10% glycerol.

Expression constructs for the human NF-κB dimers were created as established previously[44]. Briefly, histidine-tagged recombinant proteins were produced using pET vectors in BL21 (DE3) *E. coli* (Merck). Constructs contained the Rel-homology region (RHR) of each subunit: RelA (1-307 a.a.), c-Rel (1-285 a.a.), p50 (7-356 a.a.), p52 (4-332 a.a.) RelB (120-401 a.a.). Proteins expressed was induced with 0.2 mM isopropyl β-D-1-thiogalactopyranoside (IPTG) at 30 °C for 5 h. Cell pellets were harvested in “Ni-NTA Binding” buffer with added EDTA-free Protease Inhibitor (Roche), pulse-sonicated for 2 min and debris removed via centrifugation at 16,000 *g*. A two-step purification procedure was then employed, first with the “Ni-NTA His-Bind Resin” system (Merck #70666) and then a subsequent purification based on DNA-affinity isolation of functional, DNA-binding protein. Ni-NTA purification was carried according to manufacturer’s guidelines while for DNA-affinity isolation, the processing of a sample derived from 250 ml of bacterial culture required 0.128 μM of the oligonucleotides “TNF-promoter” (biotinylated) and “TNF-promoter complementary”. Oligonucleotides were annealed via incubation in NEB Buffer 3 (New England Biolabs) at 94°C for 1 min, followed by 69 cycles of 1 min with step-wise decrease of 1°C. 712.5 μl of pre-annealed oligonucleotide mixture was conjugated with streptavidin-agarose (Sigma).

PBM experiments and analysis

PBM experiments were performed using custom-designed oligonucleotide arrays (Agilent Technologies, Inc.,) Two different PBM designs were used: all 10-bp site universal PBM (Agilent Technologies Inc., AMADID #016060, 4×4K array format) described previously[26], and a custom NF-κB PBM developed as part of this study (AMADID #025227, Agilent Technologies, Inc.) DNA probe sequences synthesized on the custom-designed arrays are provided (Supplementary File 1).

Custom-designed oligonucleotide arrays (Agilent Technologies, Inc.) were converted to double-stranded DNA arrays by primer extension and used in PBM experiments as described previously[22,26]. Protein samples were incubated on the microarrays (concentrations provided, Supplementary Table 2 and 3), for 1 h in binding buffer (10 mM Tris-HCl, pH 7.4; 0.2 μg/μl bovine serum albumin (BSA) (New England BioLabs #B9001S); 0.3 ng/μl salmon testes DNA (Sigma, #D7656); 2% non-fat dry milk (Stop & Shop brand); 0.02% Triton X-100; 3 mM dithiothreitol (DTT); NaCl or KCl (salt concentrations provided, Supplementary Table 2 and 3). Protein-bound arrays were then washed and incubated with primary antibody (see Supplementary Tables 2 and 3, column 4) for 20 min. For PBM experiments in which a secondary antibody was used (see Supplementary Tables 2 and 3, column 4) we deviated from the published protocol[22] and applied an additional wash step (0.05% Tween-20/PBS for 3 min; 0.01% Triton X-100 for 2 min) before 20 min secondary antibody incubation (Supplementary Table 2 and 3, column 5).

Microarray scanning, quantification, and data normalization were performed using GenePix Pro ver. 6 (Axon) and masliner (MicroArray LINEar Regression) software as previously described[22,26]. For the custom NF-κB PBM, median fluorescence intensities for each 10-bp κB site were determined from the eight corresponding probes (forward and reverse complement orientations, four replicates each, Fig. 1a). For each PBM experiment, the median fluorescence intensity (MI) for each of the 3,285 10-bp κB sites was transformed into a z-score using the mean (u) and standard deviation (SD) derived from the median intensities values of a background set of 1,200 randomly selected 10-bp sequences also present on the PBM; i.e., z-score = (MI − u)/SD.

Surface Plasmon Resonance (SPR) experiments

Sensorgrams were recorded on a Biacore T100 (GE Healthcare) using streptavidin chips (Sensor Chip SA). Biotinylated oligonucleotide probes were immobilized on the surface of the streptavidin sensor chip in running buffer (10 mM HEPES, pH 7.5 150 mM NaCl, 3 mM EDTA, 0.005% Tween 20). Protein samples were applied to the sensor chip at 50 μL/min, at 10°C and referenced to an unmodified surface. Binding data was collected in the running buffer described above; sensor chip surface was regenerated with a 90 second pulse of 2 M NaCl followed by 180 second pulse of the running buffer. Dissociation rates were obtained by global fitting of the real-time kinetic data using the Scrubber2 software (BioLogic Software) and a simple 1:1 binding model. Six concentrations of each NF-κB protein were used, ranging from 1 nM to 1 μM.

Comparison and clustering of NF-κB PBM data

NF-κB dimer binding specificities was compared using the Pearson correlation coefficient of κB site z-scores.. Only κB sites with a z-score > 1 in at least one experiment were included in these calculations. Further, possibly redundant κB sites were ignored in the calculation if they could be explained by a higher-scoring κB site (i.e., if a higher-scoring κB 10-bp site matched its probe sequence); ~500 κB sites met this criteria. Calculations were performed using the R statistical software package. Hierarchical clustering and

visualization of the comparison matrix (Fig. 1c) were performed using the heatmap function in R, with a 'euclidean' distance function and a 'complete' clustering function.

DNA binding site motif analysis

Binding motifs for universal PBM experiments were derived using the Seed-and-Wobble algorithm[22,26]. DNA binding site motifs from top-scoring κB sites identified by custom NF-κB PBM experiments were determined by running the Priority 2.1.0 motif finding algorithm[45] on the 10-bp sequences. Graphical sequence logos were generated using enoLOGOS[46].

References

1. Baldwin AS Jr. Series introduction: the transcription factor NF-kappaB and human disease. J Clin Invest. 2001; 107:3–6. [PubMed: 11134170]
2. Tak PP, Firestein GS. NF-kappaB: a key role in inflammatory diseases. J Clin Invest. 2001; 107:7–11. [PubMed: 11134171]
3. Zhang G, Ghosh S. Toll-like receptor-mediated NF-kappaB activation: a phylogenetically conserved paradigm in innate immunity. J Clin Invest. 2001; 107:13–19. [PubMed: 11134172]
4. Hiscott J, Kwon H, Genin P. Hostile takeovers: viral appropriation of the NF-kappaB pathway. J Clin Invest. 2001; 107:143–151. [PubMed: 11160127]
5. Natoli G, Saccani S, Bosisio D, Marazzi I. Interactions of NF-kappaB with chromatin: the art of being at the right place at the right time. Nat Immunol. 2005; 6:439–445. [PubMed: 15843800]
6. Hoffmann A, Natoli G, Ghosh G. Transcriptional regulation via the NF-kappaB signaling module. Oncogene. 2006; 25:6706–6716. [PubMed: 17072323]
7. Natoli G. Tuning up inflammation: how DNA sequence and chromatin organization control the induction of inflammatory genes by NF-kappaB. FEBS Lett. 2006; 580:2843–2849. [PubMed: 16530189]
8. Bonizzi G, Karin M. The two NF-kappaB activation pathways and their role in innate and adaptive immunity. Trends Immunol. 2004; 25:280–288. [PubMed: 15145317]
9. Hayden MS, Ghosh S. Signaling to NF-kappaB. Genes Dev. 2004; 18:2195–2224. [PubMed: 15371334]
10. Gerondakis S, et al. Unravelling the complexities of the NF-kappaB signalling pathway using mouse knockout and transgenic models. Oncogene. 2006; 25:6781–6799. [PubMed: 17072328]
11. Hoffmann A, Leung TH, Baltimore D. Genetic analysis of NF-kappaB/Rel transcription factors defines functional specificities. EMBO J. 2003; 22:5530–5539. [PubMed: 14532125]
12. Chen FE, Ghosh G. Regulation of DNA binding by Rel/NF-kappaB transcription factors: structural views. Oncogene. 1999; 18:6845–6852. [PubMed: 10602460]
13. Kunsch C, Ruben SM, Rosen CA. Selection of optimal kappa B/Rel DNA-binding motifs: interaction of both subunits of NF-kappa B with DNA is required for transcriptional activation. Mol Cell Biol. 1992; 12:4412–4421. [PubMed: 1406630]
14. Udalova IA, Mott R, Field D, Kwiatkowski D. Quantitative prediction of NF-kappa B DNA-protein interactions. Proc Natl Acad Sci U S A. 2002; 99:8167–8172. [PubMed: 12048232]
15. Hoffmann A, Baltimore D. Circuitry of nuclear factor kappaB signaling. Immunol Rev. 2006; 210:171–186. [PubMed: 16623771]
16. Bonizzi G, et al. Activation of IKKalpha target genes depends on recognition of specific kappaB binding sites by RelB:p52 dimers. EMBO J. 2004; 23:4202–4210. [PubMed: 15470505]
17. Sanjabi S, et al. A c-Rel subdomain responsible for enhanced DNA-binding affinity and selective gene activation. Genes Dev. 2005; 19:2138–2151. [PubMed: 16166378]
18. Senftleben U, Li ZW, Baud V, Karin M. IKKbeta is essential for protecting T cells from TNFalpha-induced apoptosis. Immunity. 2001; 14:217–230. [PubMed: 11290332]
19. Xiao G, Harhaj EW, Sun SC. NF-kappaB-inducing kinase regulates the processing of NF-kappaB2 p100. Mol Cell. 2001; 7:401–409. [PubMed: 11239468]

20. Fusco AJ, et al. NF-kappaB p52:RelB heterodimer recognizes two classes of kappaB sites with two distinct modes. EMBO Rep. 2009; 10:152–159. [PubMed: 19098713]
21. Britanova LV, Makeev VJ, Kuprash DV. In vitro selection of optimal RelB/p52 DNA-binding motifs. Biochem Biophys Res Commun. 2008; 365:583–588. [PubMed: 17996728]
22. Berger MF, Bulyk ML. Universal protein-binding microarrays for the comprehensive characterization of the DNA-binding specificities of transcription factors. Nat Protoc. 2009; 4:393–411. [PubMed: 19265799]
23. Berger MF, et al. Compact, universal DNA microarrays to comprehensively determine transcription-factor binding site specificities. Nat Biotechnol. 2006; 24:1429–1435. [PubMed: 16998473]
24. Mukherjee S, et al. Rapid analysis of the DNA-binding specificities of transcription factors with DNA microarrays. Nat Genet. 2004; 36:1331–1339. [PubMed: 15543148]
25. Linnell J, et al. Quantitative high-throughput analysis of transcription factor binding specificities. Nucleic Acids Res. 2004; 32:e44. [PubMed: 14990752]
26. Berger MF, Bulyk ML. Protein binding microarrays (PBMs) for rapid, high-throughput characterization of the sequence specificities of DNA binding proteins. Methods Mol Biol. 2006; 338:245–260. [PubMed: 16888363]
27. Bulyk ML, Huang X, Choo Y, Church GM. Exploring the DNA-binding specificities of zinc fingers with DNA microarrays. Proc Natl Acad Sci U S A. 2001; 98:7158–7163. [PubMed: 11404456]
28. Chen YQ, Sengchanthalangsy LL, Hackett A, Ghosh G. NF-kappaB p65 (RelA) homodimer uses distinct mechanisms to recognize DNA targets. Structure. 2000; 8:419–428. [PubMed: 10801482]
29. Grilli M, Chiu JJ, Lenardo MJ. NF-kappa B and Rel: participants in a multiform transcriptional regulatory system. Int Rev Cytol. 1993; 143:1–62. [PubMed: 8449662]
30. Li Q, Verma IM. NF-kappaB regulation in the immune system. Nat Rev Immunol. 2002; 2:725–734. [PubMed: 12360211]
31. Lim CA, et al. Genome-wide mapping of RELA(p65) binding identifies E2F1 as a transcriptional activator recruited by NF-kappaB upon TLR4 activation. Mol Cell. 2007; 27:622–635. [PubMed: 17707233]
32. Kasowski M, et al. Variation in transcription factor binding among humans. Science. 2010; 328:232–235. [PubMed: 20299548]
33. Schreiber J, et al. Coordinated binding of NF-kappaB family members in the response of human cells to lipopolysaccharide. Proc Natl Acad Sci U S A. 2006; 103:5899–5904. [PubMed: 16595631]
34. Wang J, et al. Distinct roles of different NF-kappa B subunits in regulating inflammatory and T cell stimulatory gene expression in dendritic cells. J Immunol. 2007; 178:6777–6788. [PubMed: 17513725]
35. Merika M, Williams AJ, Chen G, Collins T, Thanos D. Recruitment of CBP/p300 by the IFN beta enhanceosome is required for synergistic activation of transcription. Mol Cell. 1998; 1:277–287. [PubMed: 9659924]
36. Fujita T, Nolan GP, Ghosh S, Baltimore D. Independent modes of transcriptional activation by the p50 and p65 subunits of NF-kappa B. Genes Dev. 1992; 6:775–787. [PubMed: 1577272]
37. Leung TH, Hoffmann A, Baltimore D. One nucleotide in a kappaB site can determine cofactor specificity for NF-kappaB dimers. Cell. 2004; 118:453–464. [PubMed: 15315758]
38. Cheng CS, et al. The specificity of innate immune responses is enforced by repression of interferon response elements by NF-kappaB p50. Sci Signal. 2011; 4:ra11. [PubMed: 21343618]
39. Chen YQ, Ghosh S, Ghosh G. A novel DNA recognition mode by the NF-kappa B p65 homodimer. Nat Struct Biol. 1998; 5:67–73. [PubMed: 9437432]
40. Mauxion F, Jamieson C, Yoshida M, Arai K, Sen R. Comparison of constitutive and inducible transcriptional enhancement mediated by kappa B-related sequences: modulation of activity in B cells by human T-cell leukemia virus type I tax gene. Proc Natl Acad Sci U S A. 1991; 88:2141–2145. [PubMed: 2006151]

41. Wong D, et al. Extensive characterization of NF-KappaB binding uncovers non-canonical motifs and advances the interpretation of genetic functional traits. Genome Biol. 2011; 12:R70. [PubMed: 21801342]
42. Fordyce PM, et al. De novo identification and biophysical characterization of transcription-factor binding sites with microfluidic affinity analysis. Nat Biotechnol. 2010; 28:970–975. [PubMed: 20802496]
43. Rucker P, Torti FM, Torti SV. Recombinant ferritin: modulation of subunit stoichiometry in bacterial expression systems. Protein Eng. 1997; 10:967–973. [PubMed: 9415447]
44. Field S, Udalova I, Ragoussis J. Accuracy and reproducibility of protein-DNA microarray technology. Adv Biochem Eng Biotechnol. 2007; 104:87–110. [PubMed: 17290820]
45. Gordan R, Narlikar L, Hartemink AJ. Finding regulatory DNA motifs using alignment-free evolutionary conservation information. Nucleic Acids Res. 38:e90. [PubMed: 20047961]
46. Workman CT, et al. enoLOGOS: a versatile web tool for energy normalized sequence logos. Nucleic Acids Res. 2005; 33:W389–392. [PubMed: 15980495]

Europe PMC Funders Author Manuscripts

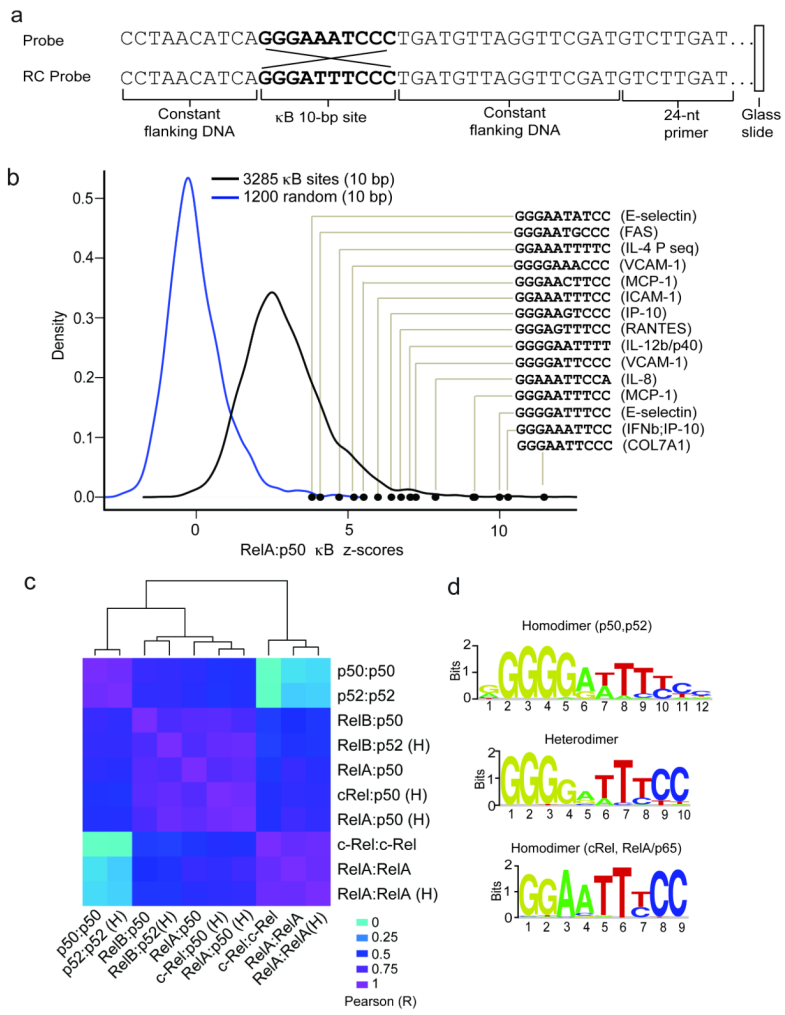

Figure 1.

Examining NF-κB dimer binding by custom NF-κB PBMs. (**a**) Schematic of design of 60 base-pair (bp) DNA sequence probes on custom NF-κB PBM. 10-bp κB sites are positioned at a fixed position along the probe (i.e., relative to the glass slide surface) within constant flanking sequence. Each 10-bp κB site is present at four replicate spots in both the forward ('Probe') and reverse complement ('RC Probe') orientation (i.e., eight spots in total). (**b**) Distributions of PBM-derived binding site z-scores for mouse RelA:p50 binding to 3,285 κB sites (black line) and to a background set of 1,200 random 10-bp sequences (blue line). Z-scores for 15 κB sites described in the literature are indicated. (**c**) Pair-wise comparison of κB site binding for 10 NF-κB dimers. Pair-wise binding similarity was assessed by Pearson correlation of κB site z-scores, and hierarchical clustering was performed on the comparison matrix (see Methods). Three DNA-binding specificity clusters (i.e., class) were identified that correspond to three NF-κB dimer groups: p50,p52 homodimers, heterodimers and c-Rel,RelA homodimers. Representative DNA binding site motifs were determined for each dimer class using the top 25 highest-scoring κB sites bound by each group member (Methods; see Supplementary Fig. 2 for individual motifs).

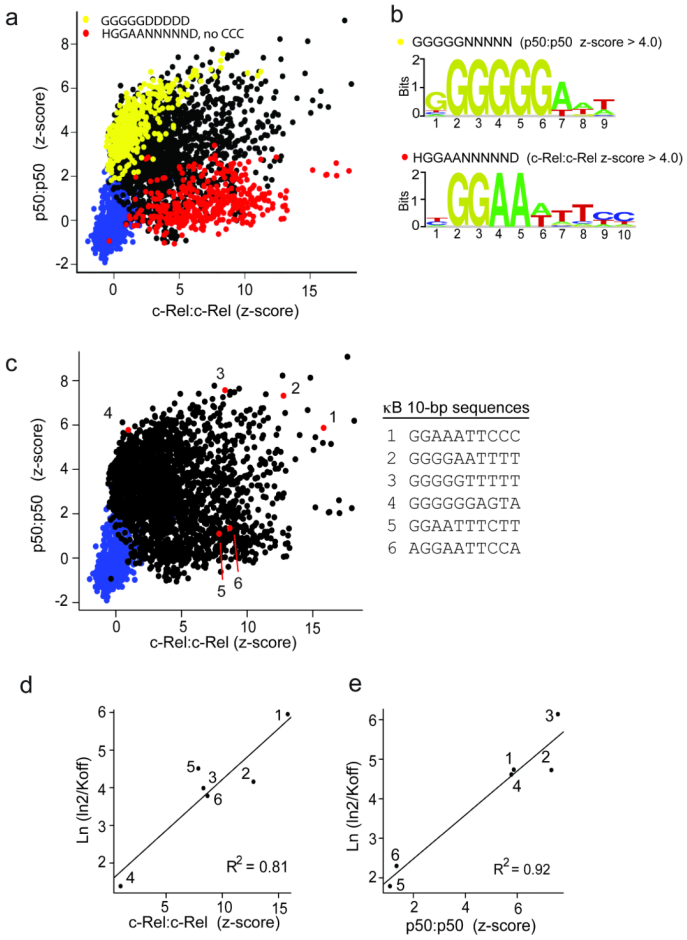

Figure 2.

Dimer-specific binding to traditional and non-traditional κB sites. (**a**) Comparison of the binding by mouse p50:p50 and c-Rel:c-Rel homodimers to 3,285 κB sites (black dots) and a background set of 1,200 random 10-bp sites (blue dots). κB sites conforming to the patterns 5′-GGGGGNNNNN-3′ (N = any base) and 5′-HGGAANNNNND-3′ (H = not G, D = not C, NNNNN = all 5-bp sequences except those containing CCC triplets) are highlighted in yellow and red, respectively. Binding motifs specific for subsets of κB sites are shown. (**b**) Z-scores and DNA sequences of six κB sites used in subsequent SPR experiments (see (c) and (d) below and Table 1) are shown. (**c**),(**d**) Comparison of SPR-determined binding off-rates (K_{off}) and PBM-determined z-scores are shown for c-Rel:c-Rel and p50:p50 homodimers, respectively.

Europe PMC Funders Author Manuscripts

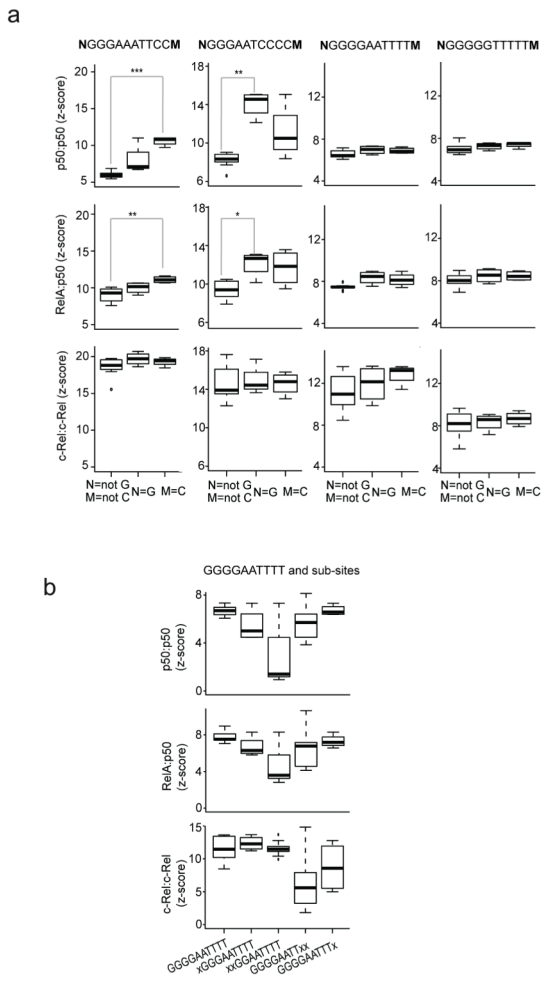

Figure 3.

Preferences for flanking DNA bases and κB site length. (**a**) Z-score distributions are shown for 10-bp κB sites with different flanking bases (e.g. identity of N and M in NGGGAATCCCCM). In each panel, column 1 has scores for κB sites with no 5′ guanine (forward orientation, N = not G; reverse complement orientation, M = not C); column 2 has scores for κB sites with 5′ guanine (N = G); column 3 has scores for κB sites with 5′ guanine in reverse complement orientation (M = C). κB sites for which a 5′ guanine flanking base (column 2 or 3) results in significantly higher z-scores (p-value < 0.01, one-tailed Student's t-test) are indicated (10^{-4} (***), 10^{-3} (**), 10^{-2} (*)). Data are shown for PBM experiments performed for p50:p50, RelA:p50 and c-Rel:c-Rel. (**b**) Z-score distributions are shown for the non-traditional 10-bp κB site 5′-GGGGAATTTT-3′ and shorter variant sites. Score distribution for 10-bp sites are as in (a). Score distributions for shorter sites are determined by examining scores from all κB sites in our dataset that contained the sub-site sequence. For example, column 2 labeled xGGGAATTTT has scores from the 4 κB sites where x = A,C,G or T.

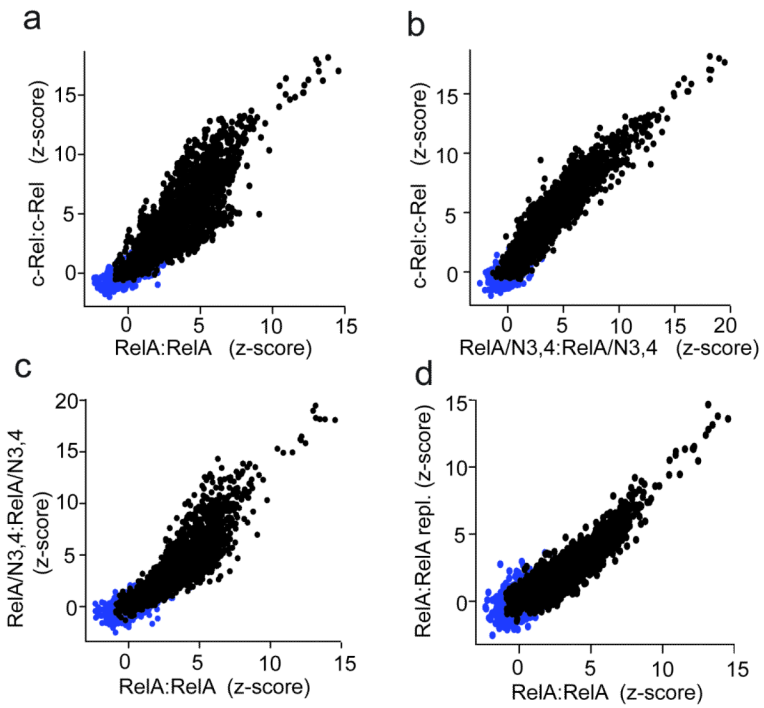

Figure 4.

Comparison of c-Rel, RelA and RelA/N3,4 homodimer DNA-binding specificity. (**a**) Comparison of the binding by mouse c-Rel:c-Rel and RelA:RelA homodimers to 3,285 κB sites (black dots) and a background set of 1,200 random 10-bp sites (blue dots). (**b**) Comparison for c-Rel:c-Rel and RelA/N3,4:RelA/N3,4. (**c**) Comparison for RelA/N3,4:RelA/N3,4 and RelA:RelA. (**d**) Comparison for RelA:RelA (replicate experiment) and RelA:RelA.

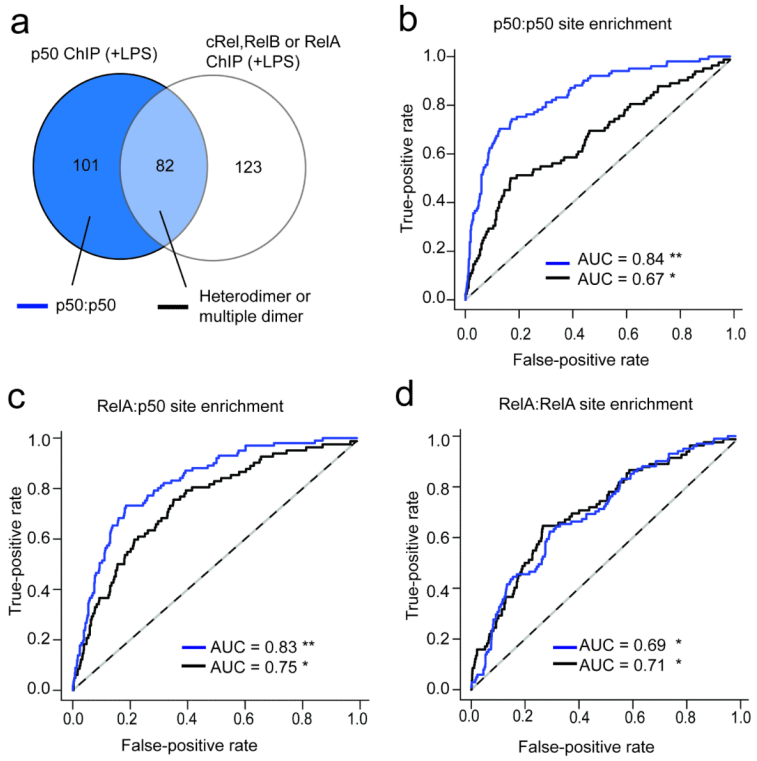

Figure 5.

Enrichment of PBM-determined κB sites in published dataset of p50-bound genomic regions from LPS-stimulated human macrophages[33]. **(a)** Venn diagram showing the overlap of 183 p50-bound regions with the 205 regions bound by c-Rel, RelB or RelA. Bound regions are the ChIP enriched regions (p-value < 0.002) reported in Figure 1 of Schreiber *et al.* (**b,c,d**) Receiver operating characteristic (ROC) curve analyses quantifying the enrichment within p50-bound regions of PBM-determined κB sites are shown for (b) p50, (c) RelA:p50, and (d) RelA. ROC curves describe enrichment within p50-specifically bound regions (blue line), and within regions bound by p50 and at least one of cRel, RelB, or RelA (black line). Area under the ROC curve (AUC) values are reported to quantify the enrichment, and a Wilcox-Mann-Whitney U test was applied to calculate the significance of each AUC value.

Europe PMC Funders Author Manuscripts

Europe PMC Funders Author Manuscripts

Table 1

SPR-determined dissociation half-life values ($t_{1/2}$) for different NF-κB dimers and κB sites. Half-life values, directly proportional to dissociation off-rates ($t_{1/2} = \ln(2)/K_{off}$, standard deviation in brackets), are listed for six different 10-bp κB site sequences (Fig. 2), and for four different mouse NF-κB dimers (Columns 3-6). The variant RelA/N3,4:RelA/N3,4 is a homodimer of the previously described RelA mutant[17].

	Sequence	Probe ID	p50:p50 (sec)	c-Rel:c-Rel (sec)	RelA;RelA (sec)	RelA/N3,4:RelA/N3,4 (sec)
1	GGAAATTCCC	p65-7	120 (27)	367 (54)	45 (1)	115 (17)
2	GGGGAATTTT	p40 orig	113 (12)	64 (2)	7 (2)	25 (1)
3	GGGGGTTTTT	PBM2	437 (77)	58 (11)	7 (1)	28 (6)
4	GGGGGGAGTA	PBM3	91 (27)	4 (1)	4 (1)	8 (5)
5	GGAATTTCTT	CD28RE	6 (0.2)	92 (10)	3 (1)	39 (2)
6	AGGAATTCCA	PBM1	9 (2)	46 (8)	1 (0.3)	22 (3)

Europe PMC Funders Author Manuscripts

Table 2

Principles of regulatory specificity for NF-κB dimer classes.

c-Rel:c-Rel, RelA:RelA Homodimers
Highly correlated binding profiles
Selective activation by c-Rel:c-Rel achieved via enhanced binding affinity[17]
Selective activation by RelA:RelA may require interactions with co-regulatory proteins[34]
Heterodimers
Highly correlated binding profiles
Selective activation by each heterodimer may require interactions with co-regulatory proteins
p50:p50, p52:p52 Homodimers
Highly correlated binding profiles
Non-traditional, G-rich sites support preferential binding by these dimers and confer dimer-specific regulatory functions[38]
All dimers
Binding to varied DNA sites (e.g. different lengths, one degenerate half-site) that correlates with structural differences of DNA-bound complexes may facilitate allosteric regulatory mechanisms[36,37]